ORIGINAL RESEARCH

Rotigaptide Infusion for the First 7 Days After Myocardial Infarction–Reperfusion Reduced Late Complexity of Myocardial Architecture of the Healing Border-Zone and Arrhythmia Inducibility

Rasheda A. Chowdhury (iD), PhD; Michael T. Debney, MBBS, PhD; Andrea Protti, PhD; Balvinder S. Handa (iD), MBBS; Kiran H. K. Patel, MBBS; Alexander R. Lyon, BM BCh, PhD; Ajay M. Shah (iD), MB BCh; Fu Siong Ng (iD), MBBS, PhD; Nicholas S. Peters (iD), MBBS, MD

BACKGROUND: Survivors of myocardial infarction are at increased risk of late ventricular arrhythmias, with infarct size and scar heterogeneity being key determinants of arrhythmic risk. Gap junctions facilitate the passage of small ions and morphogenic cell signaling between myocytes. We hypothesized that gap junctions enhancement during infarction–reperfusion modulates structural and electrophysiological remodeling and reduces late arrhythmogenesis.

METHODS AND RESULTS: Infarction–reperfusion surgery was carried out in male Sprague-Dawley rats followed by 7 days of rotigaptide or saline administration. The in vivo and ex vivo arrhythmogenicity was characterized by programmed electrical stimulation 3 weeks later, followed by diffusion-weighted magnetic resonance imaging and Masson's trichrome histology. Three weeks after 7-day postinfarction administration of rotigaptide, ventricular tachycardia/ventricular fibrillation was induced on programmed electrical stimulation in 20% and 53% of rats, respectively (rotigaptide versus control), resulting in reduction of arrhythmia score (3.2 versus 1.4, $P=0.018$), associated with the reduced magnetic resonance imaging parameters fractional anisotropy (fractional anisotropy: −5% versus −15%; $P=0.062$) and mean diffusivity (mean diffusivity: 2% versus 6%, $P=0.042$), and remodeling of the 3-dimensional laminar structure of the infarct border zone with reduction of the mean (16° versus 19°, $P=0.013$) and the dispersion (9° versus 12°, $P=0.015$) of the myofiber transverse angle. There was no change in ECG features, spontaneous arrhythmias, or mortality.

CONCLUSIONS: Enhancement of gap junctions function by rotigaptide administered during the early healing phase in reperfused infarction reduces later complexity of infarct scar morphology and programmed electrical stimulation–induced arrhythmias, and merits further exploration as a feasible and practicable intervention in the acute myocardial infarction management to reduce late arrhythmic risk.

Key Words: gap junction ■ infarct heterogeneity ■ rotigaptide ■ ventricular arrhythmias

---

Survivors of myocardial infarction (MI) are at high risk of sudden cardiac death because of the elevated long-term incidence of fatal ventricular arrhythmias including ventricular tachycardia (VT) and ventricular fibrillation (VF).[1] In the late, healed phase of MI, the presence of scar and a disorganized interface between normal and infarcted myocardium, the infarct border zone (IBZ), provide the conditions necessary

<div style="border:2px solid red; padding:10px;">

CLINICAL PERSPECTIVE

What Is New?
- Early gap junction enhancement reduces late complexity of infarct scar.
- These changes can be identified using magnetic resonance indices.

What Are the Clinical Implications?
- There is a potential therapeutic value of rotigaptide treatment alongside reperfusion strategies in acute management of postmyocardial infarction.

</div>

<div style="border:2px solid red; padding:10px;">

Nonstandard Abbreviations and Acronyms

CL	cycle length
CON	control group
FA	fractional anisotropy
GJ	gap junction
HA	helix angle
MD	mean diffusivity
ROT	rotigaptide group
S1S2	extrastimulus provocation protocol
SHAM	sham group
TA	transverse angle

</div>

to initiate and sustain ventricular arrhythmias.[2] Infarct size[3,4] and the extent of the peri-infarct, heterogeneous IBZ[5] are both independent predictors of the incidence of VT and VF.

Current strategies to reduce the incidence[6,7] of VT/VF and prevent sudden cardiac death include long-term anti-arrhythmic drugs[8] that have limited efficacy, such that cardioverter-defibrillators[9] are widely implanted to treat, rather than prevent, VT and VF with significant procedural and device complications and high financial costs.[10]

Electrophysiological remodeling occurs during ischemia–reperfusion and increases arrhythmia susceptibility.[11] Cardiac gap junctions (GJ) have an important role in the safe spread of electrical activity in normal myocardium[12] and we have previously shown that not only is GJ remodeling arrhythmogenic because of the effects on conduction promoting reentry in animal models of infarction,[13,14] but distinct from this, we have also shown that gap-junctional coupling at the time of infarction also has a role in modeling the architecture of the late healed IBZ,[15] likely because of the acute effects of the passage of ions and small molecules that mediate cell death or survival.[16] Furthermore, the opposing "kiss-of-life"

and "kiss-of-death" hypotheses, referring to the intracellular spread of either cell-survival or apoptotic signals, respectively, suggest that the degree of passage of signaling factors via open GJ channels between adjacent myocytes determines the eventual extent of cellular injury.[17]

Administration of pharmacological agents that enhance GJ coupling (eg, rotigaptide,[18] danegaptide[19]) in the early (<4 hour) phase post-MI[20,21] in large-animal models have consistently demonstrated an acute anti-arrhythmic effect as a result of enhanced conduction during ischemia. This is thought to occur via the suppression of dephosphorylation of the GJ protein connexin43 at Ser297 and Ser368 following 30 minutes ischemia.[22] Because of the ability of gap junctional channels to allow the passage of apoptotic signals, in addition to small ions, their role in the spread of infarction has been queried.[17] Rotigaptide has not been shown to attenuate ischemia-induced connexin43 lateralization.[15]

In the rodent chronic MI model, rotigaptide administered peri-MI also resulted in a small reduction in infarct size measured in the late phase (3 weeks) post-MI.[23] However, any reduction in infarct size in this and other studies is minimal (<10%), thereby having negligible potential to modulate tissue mechanics and improve left ventricular (LV) function. Given that arrhythmogenesis of the healed border zone depends on tissue microarchitecture, any effect at the microstructural level may profoundly affect arrhythmogenesis—the concept underpinning this hypothesis requiring the detailed histomorphometry and in vivo magnetic resonance imaging (MRI) of the myocardium as presented in this study.

Remodeling of the infarct region post-MI has been characterized with diffusion MRI (specifically diffusion tensor imaging) in a range of experimental[24,25] and clinical[26,27] studies. The majority have shown fractional anisotropy (FA) to decrease (ie, fiber architecture becomes more disordered and less anisotropic) both adjacent to and in infarcted regions, associated with an increase in mean diffusivity (MD) [24,26,28] attributed to cell necrosis, edema, and loss of cellularity. The influence of rotigaptide on fiber architecture remodeling has not previously been studied.

We, therefore, hypothesized that early enhancement of GJ coupling during infarction–reperfusion modulates subsequent infarct healing by reducing structural heterogeneity of the border zone, resulting in a myocardial substrate less prone to late arrhythmogenesis.

METHODS

Methods are described briefly here with extended methods available in Data S1. The data that support

the findings of this study are available from the corresponding author upon reasonable request.

Animal Studies

All animal procedures were performed in accordance with the standards set out in the UK Animals (Scientific Procedures) Act 1986 and EU 2012 with appropriate Home Office permissions and local ethical review board approval. Thirty-seven male Sprague Dawley rats (weight 250–350 g) underwent myocardial infarction–reperfusion surgery[29] (60 minutes of left anterior descending artery occlusion) before being studied at 4 weeks recovery. Animals were randomly divided into 2 groups at the time of MI surgery: a control group (CON) that received phosphate-buffered saline and a treatment group that received the GJ-enhancing drug rotigaptide (ROT). Drug dosing consisted of an initial intraperitoneal bolus at 15 minutes post-MI (ROT dose 2.5 mol/kg, phosphate-buffered saline dose 1 mL) followed by 7 days of administration via osmotic minipump (Pump 2ML1, Azlet) implanted into the abdominal cavity (rotigaptide rate 0.11 nmol/kg per day,[23] phosphate-buffered saline rate 2 mL/wk). Five sham-ligated (SHAM) animals acted as non-MI, nondrug controls.

In Vivo Electrophysiological Studies

The incidence of spontaneous arrhythmias (ventricular premature beats, VT, and VF) was recorded using a wireless ECG telemetry transmitter (CA-F40, Data Sciences International) implanted into the abdominal cavity. Arrhythmias were quantified over a 24-hour period at 4 weeks post-MI and a composite arrhythmia score was calculated.[30] Resting ECG intervals (RR, PR, QRS, and QTc[31]) were measured at 4 weeks post-MI by recording a resting 6-lead ECG with animals under light general anesthesia.

Ex Vivo Electrophysiological Studies

At 4 weeks post-MI, hearts were explanted and Langendorff perfused with oxygenated Krebs-Henseleit buffer.[32] Susceptibility to programmed arrhythmias was tested by performing an extrastimulus provocation protocol (S1S2)[33] with the incidence of induced arrhythmias recorded and a validated arrhythmia score calculated.[34] Briefly, hearts were subject to an S1S2 extrastimuli provocation protocol with a drivetrain of 10 beats (S1) at a cycle length (CL) of 120 ms followed by introduction of a premature extra stimulus (S2) at a shorter CL. This shorter CL started at 100 ms and decremented by 2 ms until the heart was refractory and failed to capture. If the heart remained in sinus rhythm at the end of the S1S2 protocol, an S1S2S3 protocol was performed with a drivetrain of 10 beats (S1) at a CL of 120 ms, a fixed interval premature S2 stimuli at 100 ms, then a variable premature S3 stimuli starting at 80 ms and decremented by 2 ms until the heart was refractory. ECG and pacing data were recorded continuously for offline analysis.

Dual optical mapping of voltage and calcium transients was performed on the epicardial surface[35] at a baseline pacing CL of 150 ms and conduction velocity, upstroke kinetics (time of maximum change in fluorescence, rise time), action potential, and calcium transient duration (at 50%, 75%, and 90% repolarization) calculated as previously described.[36]

Infarct Size Quantification

Following optical mapping, hearts were perfusion fixed with 10% Formalin and sectioned at 1-mm spacing encompassing the entire LV (10–14 sections per heart) before Masson's trichrome staining to delineate infarct from normal myocardium and to allow area-based planimetric quantification of infarct size.

Diffusion Tensor Imaging

After completion of ex vivo studies, hearts were removed from the Langendorff perfusion apparatus and the aorta was recannulated with a 1.2-mm stainless steel cannula. Hearts were first perfused with a heparinized, high K+ KHB solution (20 mmol/L of K+) to arrest the heart in end-diastole before being attached to a 50-mL syringe pump (VWI International, UK), containing 10% neutral buffered formalin. The heart was perfusion fixed with 10% neutral buffered formalin at a rate of 10 mL/min for 10 minutes (total volume 100 mL) before storage in a 20-mL universal tube (VWR International Ltd, UK) of 10% neutral buffered formalin to allow for immersion fixation. The atria were removed using a razor blade to form a flat surface in the short-axis plane for spatial reference. Fixation was commenced within 2 minutes of cessation of perfusion so as to minimize the effective postmortem interval time.

Diffusion tensor imaging was performed using a 7.0T MRI system (Agilent, Palo Alto, CA) with 100 G/cm gradients running VNMRJ 3.2 with a 33-mm quadrature RF coil. A diffusion-sensitized fast-spin echo sequence was used to acquire diffusion-weighted data in 6 directions (Jones 6 diffusion[37] scheme at a b-value of 1000 s/mm^2 with a total of 6 spatial averages). Data were reconstructed offline using validated software (Diffusion Toolkit[38]) to fit the diffusion tensor and extract 2 measures of tissue architecture: FA and MD. Helix (HA) and transverse angles (TA) were calculated from the orientation of the primary eigenvector as previously described.[39]

FA is a measure of tissue anisotropy and is a normalized, scalar measure of the degree of anisotropy within a voxel. MD is a measure of the overall diffusivity of a voxel, independent of anisotropy, and is affected by cellular size and integrity. HA and TA are eigenvectors that define the diffusion ellipsoid profile for each voxel. HA was defined as the angle subtended between (1) the projection of the primary eigenvector onto the tangential plane and (2) the transverse plane. TA was defined as the angle subtended between the projection of the primary eigenvector onto the transverse plane and the tangential plane.

Data Analysis and Statistical Analysis

ANOVA tests were used to compare means between multiple groups with post hoc Tukey test if ANOVA was significant. Student t tests were used to compare means between 2 groups. The assumption of normality underlying both ANOVA and t tests was reasonable for the outcomes being examined. A P value of <0.05 was considered significant. All values are presented as rotigaptide versus control mean±SEM unless otherwise stated. The statistical software used was GraphPad Prism v5.

RESULTS

Survival and Weight

Survival to end of study-protocol (28 days) was similar in both treatment groups (15/18 versus 15/19, ns). Body weight at end of study-protocol was equal between groups (421±33 g versus 414±14 g, ns) with no difference in weight gain over the study period (158±8 g versus 151±8 g, ns).

Rotigaptide Reduces Arrhythmogenicity in Reperfused Infarcted Myocardium After Programmed Stimulation

Sixty minutes of infarction followed by reperfusion increased the incidence of spontaneous ventricular arrhythmias measured in the late, healed phase of infarction (number of ventricular premature beats/d CON [n=15] 1866±1513 versus SHAM [n=5] 4±1, $P<0.001$). Administration of rotigaptide before reperfusion and for the first week post-MI did not reduce the incidence of spontaneous ventricular premature beats (ROT [n=15] 1736±630, ns), nor did rotigaptide reduce the 24-hour composite arrhythmia score (2.6±0.3 versus 2.0±0.2, ns, Figure 1). Resting 6-lead ECG parameters (PR, QRS, RR, QTc intervals) measured in the late, healed phase of infarction were similar across all groups (Table 1).

Rotigaptide treatment had a significant antiarrhythmic effect in reducing the susceptibility to ex vivo programmed stimulation (arrhythmia score 1.4±0.4 versus 3.2±0.6, $P=0.018$), driven by a reduction in the inducibility of sustained VT/VF (proportionally 20% versus 53% in each group, Figure 2). No arrhythmias were inducible in sham-operated animals. Optical recordings showed CLs of <100 ms and a variety of action potential morphologies (Figure 3).
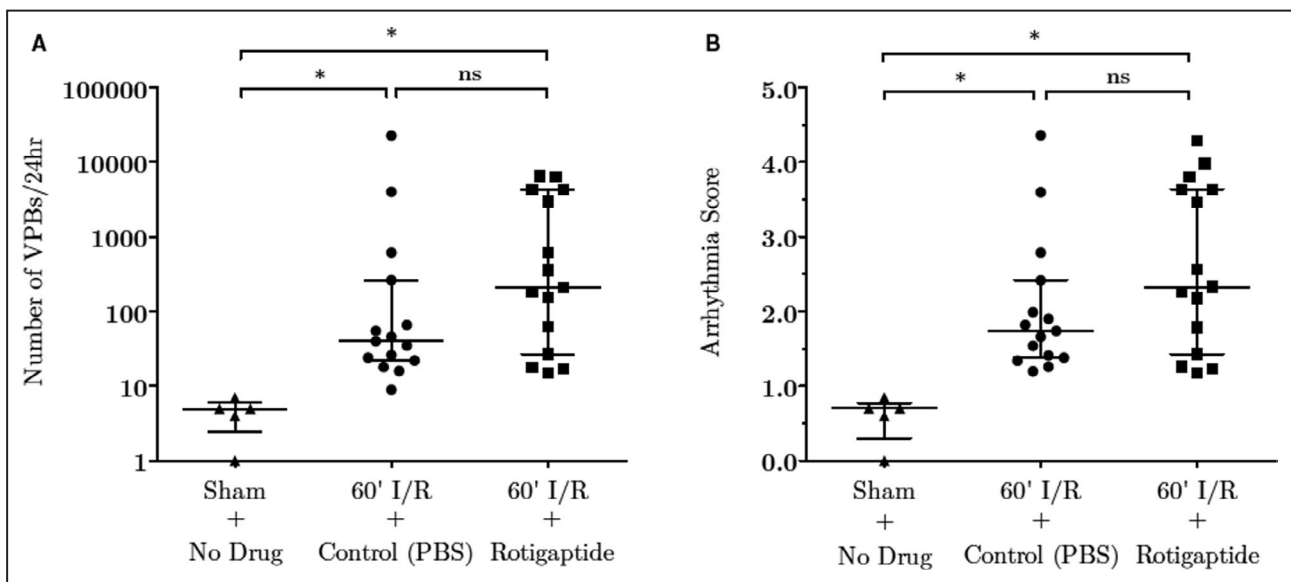

Figure 1. **Incidence of spontaneous ventricular arrhythmias recorded at the end of the healed phase (day 28) post-myocardial infarction (MI) surgery.**
A, Number of ventricular premature beats (VPB) occurring during 24-hour period. **B**, Composite arrhythmia score including VPB, ventricular tachycardia, and ventricular fibrillation occurring during 24-hour period. Sham=sham-operated (n=5), MI+CON=control (n=15), MI+ROT=rotigaptide (n=15). I/R indicates infarction/reperfusion; ns, not significant; and PBS, phosphate-buffered saline. *$P<0.05$.

ECG Interval (ms)	Sham	MI+CON	MI+ROT	*P* Value
PR	47±3	49±4	48±4	0.221*
QRS	26±1	28±3	29±4	0.474*
QTc	74±5	76±7	75±8	0.863*
RR	168±5	164±10	167±9	0.423*

Resting ECG parameters (PR interval, QRS duration, corrected QT [QT$_c$] interval, and RR interval, in milliseconds [ms]) measured at the end of the healed phase (28 days) post-myocardial infarction (MI). CON indicates MI+control; ROT, MI+rotigaptide-treated; and Sham, sham-operated.

*ns, not significant.

Rotigaptide Did Not Alter Conduction Velocities, Action Potential, or Calcium Transient Kinetics in Reperfused Infarcted Myocardium

Conduction velocities (CV) in remote myocardium of CON hearts were significantly lower compared with sham-operated (CON [n=12] 62.5±2.6 cm/s versus SHAM [n=5] 80.0±5.0 cm/s, *P*=0.021) but similar to rotigaptide-treated ([n=13] 65.7±3.6, ns). The conduction velocities at the infarct border zone were similar between control and ROT groups (50.9±2.7 versus 54.1±3.0 cm/s, ns), as was the percentage reduction in conduction velocities from remote (29.5±7.5% versus 10.8±5.5%, ns) (Figure 4A).

Action potential rise time was significantly prolonged in the infarct region compared with remote (CON 11±2 ms versus 5±1 ms, *P*<0.001, ROT 12±4 versus 6±1 ms, *P*=0.007) with no difference between treatment groups. The maximal rate of action potential upstroke, time of maximum change in fluorescence, was significantly reduced in the infarct region compared with remote (CON 0.13±0.01 arbitrary units (AU)/s versus 0.16±0.01 AU/s, *P*<0.001, ROT 0.13±0.01 AU/s versus 0.16±0.01 AU/s, *P*=0.003) with no difference between treatment groups. Rise time and time of maximum change in fluorescence in sham-operated hearts were similar to the remote region of control and rotigaptide-treated hearts (rise time 5±1 ms, ns versus CON and ROT, time of maximum change in fluorescence 0.17±0.01 AU/s, s versus CON and ROT) (Figure 4B).

Action potential duration (APD) and calcium transient duration were similar in remote regions across all groups with a significant prolongation of APD$_{50}$ in the infarct region in both control and ROT groups (Table 2).
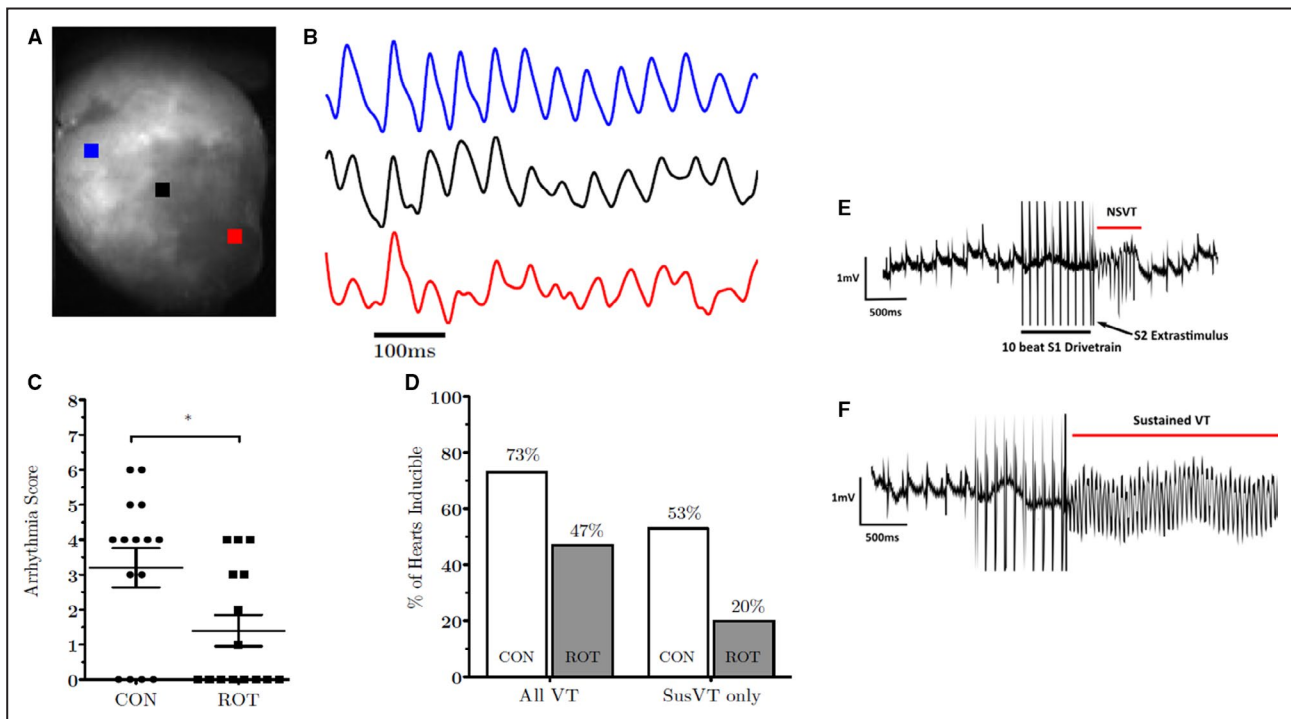

Figure 2. Representative optical action potential recordings during PES-induced VT/VF and susceptibility to arrhythmias studied ex vivo at the end of the healed phase (day 28) post-MI.
A, Black-and-white image represents visible epicardial optical mapping surface with (**B**) 3 action potential transients showing rapid (CL <100 ms) tachyarrhythmia voltage recordings from remote (blue), infarct border zone (black), and infarct (red) myocardium. **C**, Arrhythmia score from extrastimulus arrhythmia provocation studies. **D**, Incidence of VT (encompassing both sustained and nonsustained VT) induced by extrastimulus arrhythmia provocation studies. Sham+no drug=sham operated (n=5), MI+CON=control (n=15), MI+ROT=rotigaptide (n=15). *P<0.05 (**E**) ECG example of nonsustained VT. (**F**) ECG example of sustained VT. CL indicates cycle length; CON, control; MI, myocardial infarction; NSVT, nonsustained ventricular tachycardia; PES, programmed electrical stimulation; ROT, rotigaptide; SUS, sustained; VF, ventricular fibrillation; and VT, ventricular tachycardia.
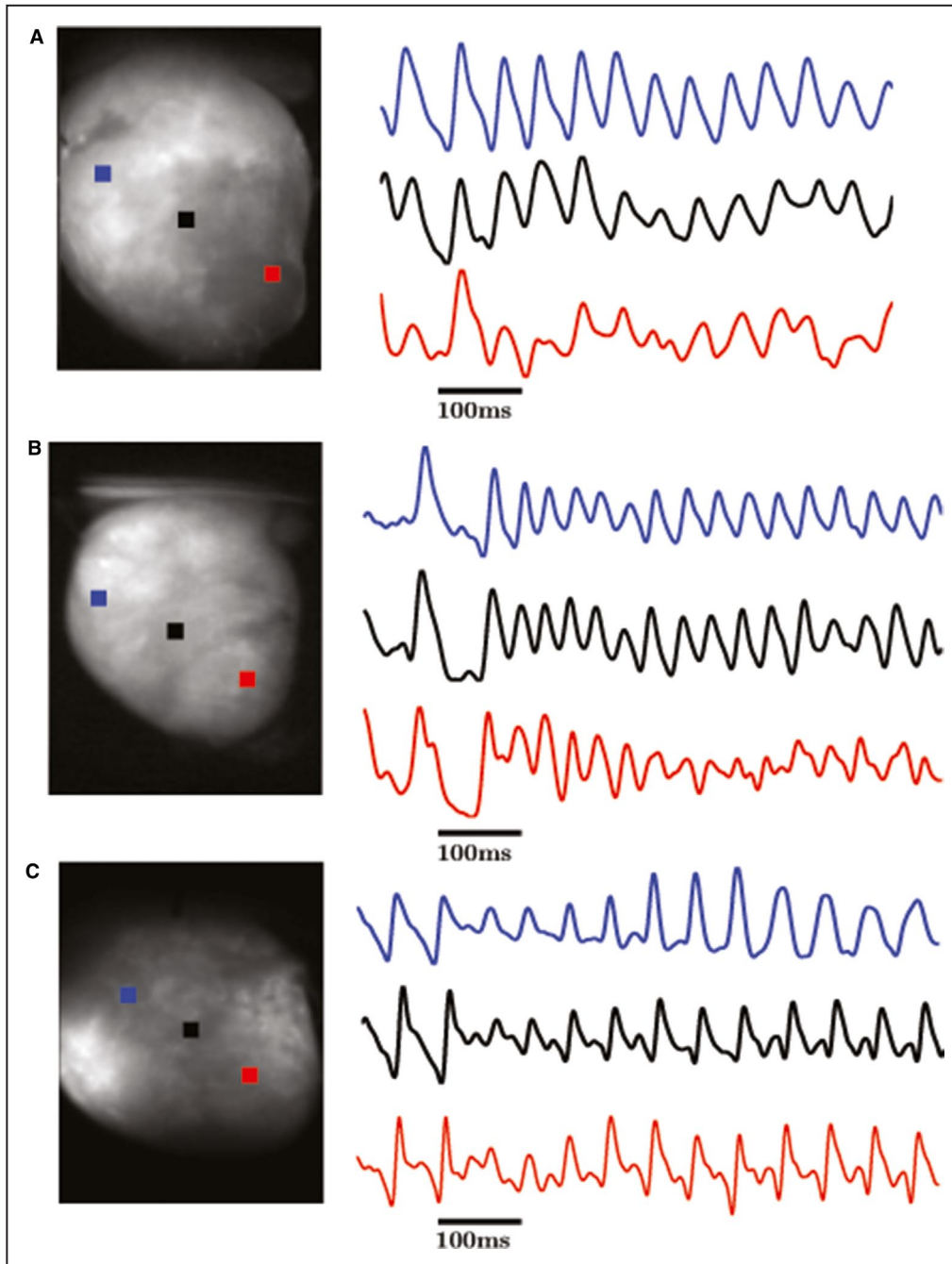
Figure 3. **Representative optical action potential recordings during premature extra stimulus–induced VT/VF.**

Three examples (**A** through **C**) of sustained VT/ VF recorded during programmed electrical stimulation. Black-and-white image represents visible epicardial optical mapping surface with 3 action potential transients showing rapid (CL <100 ms) tachyarrhythmia voltage recordings from normal (blue), infarct border zone (black), and infarct (red) myocardium. CL indicates cycle length; VF, ventricular fibrillation; and VT, ventricular tachycardia.

Rotigaptide Reduced Diffusion-MRI-Derived Indices of Tissue Heterogeneity in the Infarct Region Without Altering Infarct Size

For validation of the accuracy of the MR parameters, qualitative comparison with histology demonstrated a clear visual relationship between areas of low fractional anisotropy, high MD, and areas of collagen (scar) on Masson's trichrome staining (Figure 5). The consistency between histological and MR values was further quantified. The mean Euclidean distance between histology and MRI point-sets postregistration was 1.27±0.11 pixels
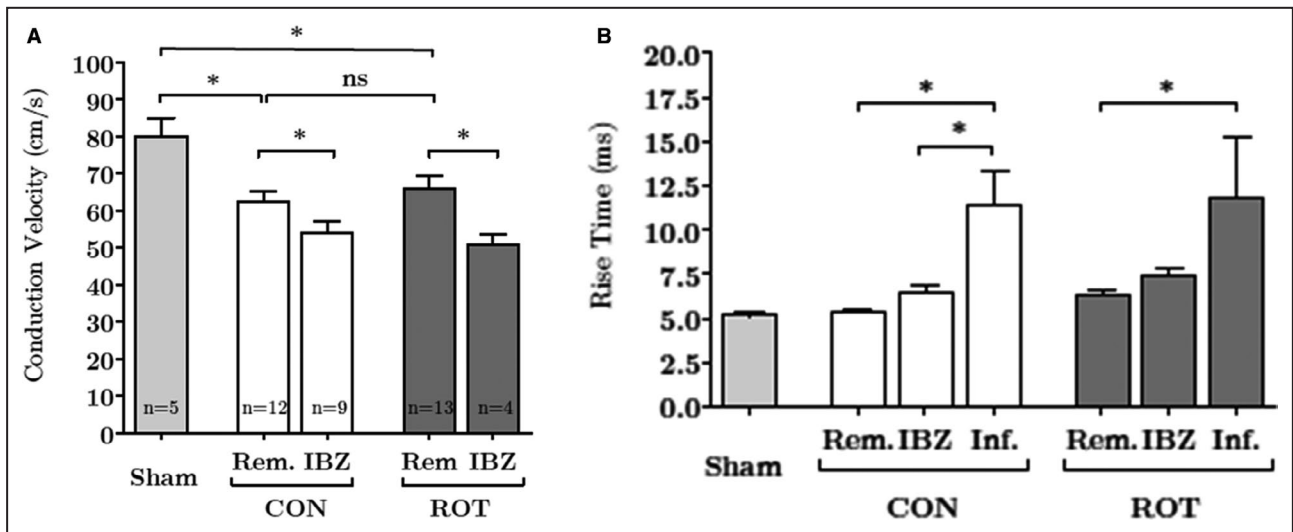
Figure 4. Effects of rotigaptide on CV and action potential rise time.
A, Reduction in CV at IBZ, comparable between treatment groups. **B**, Prolongation of rise time in the infarct region, comparable between treatment groups. CON indicates control; CV, conduction velocity; IBZ, infarct border zone; ns, not significant; Rem, remote; and ROT, rotigaptide. *$P<0.05$.

(from n=20 registrations), indicating good coregistration between images using the methods described. There was agreement between the orientations of myocardium calculated from histology, compared with the orientation calculated from the 2-dimensional primary eigenvector with a mean error of 9.5±2.3° (Figure 5), in keeping with previous literature values.[40]

Rotigaptide did not reduce infarct size measured at 28 days post-MI (12.2±1.7% versus 17.3±2.9%, $P=0.16$, Figure 6), nor did it reduce the proportion of hearts demonstrating full-thickness transmural infarct extension (29% versus 60%, $\chi^2=0.09$) or significant infarct thinning (defined as thickness <50% of remote region, 14% versus 27%, $\chi^2=0.41$).

FA and MD were compared on a region-by-region basis (remote, IBZ, and infarct) for control and rotigaptide-treated hearts. In control hearts (n=4), FA was significantly reduced in the infarct region relative to remote (−15±6%, $P=0.006$ versus remote), whereas in rotigaptide-treated hearts (n=3) the reduction in FA failed to reach statistical significance (−5±3%, ns versus remote, Figure 6). In control hearts, mean diffusivity was significantly increased in the infarct region relative to remote (6±2%, $P=0.042$ versus remote), whereas in rotigaptide-treated hearts the increase in MD failed to reach statistical significance (2±1%, ns versus remote, Figure 6).

HA demonstrated a smooth transition from endocardium (right-handed helix, +90°) to epicardium

Table 2. APD and CaTD Parameters

		AP Duration (ms)			CaT Duration (ms)		
		APD$_{50}$	APD$_{75}$	APD$_{90}$	CaTD$_{50}$	CaTD$_{75}$	CaTD$_{90}$
Remote region	Sham	26±2	53±4	72±6	51±4	70±4	79±6
	Control	27±2	51±4	70±3	44±2	65±2	78±2
	Rotigaptide	26±1	48±3	66±3	46±2	66±2	78±2
ANOVA (P value)		0.967	0.776	0.345	0.172	0.479	0.965
IBZ region	Control	29±2	51±4	71±4	48±3	66±3	77±3
	Rotigaptide	33±3	55±4	73±4	52±4	69±5	80±5
t test (P value)		0.318	0.502	0.738	0.464	0.550	0.530
Infarct region	Control	38±4*	58±4	74±3	49±3	65±3	76±2
	Rotigaptide	34±6†	57±5	76±3	47±3	64±3	74±3
t test (P value)		0.609	0.951	0.722	0.560	0.908	0.667

Effect of rotigaptide treatment on action potential (APD) and calcium transient duration (CaTD) at 50%, 75%, and 90% of repolarization in remote, infarct border zone (IBZ), and infarct regions.
*$P<0.05$ vs APD$_{50}$ in remote region of control.
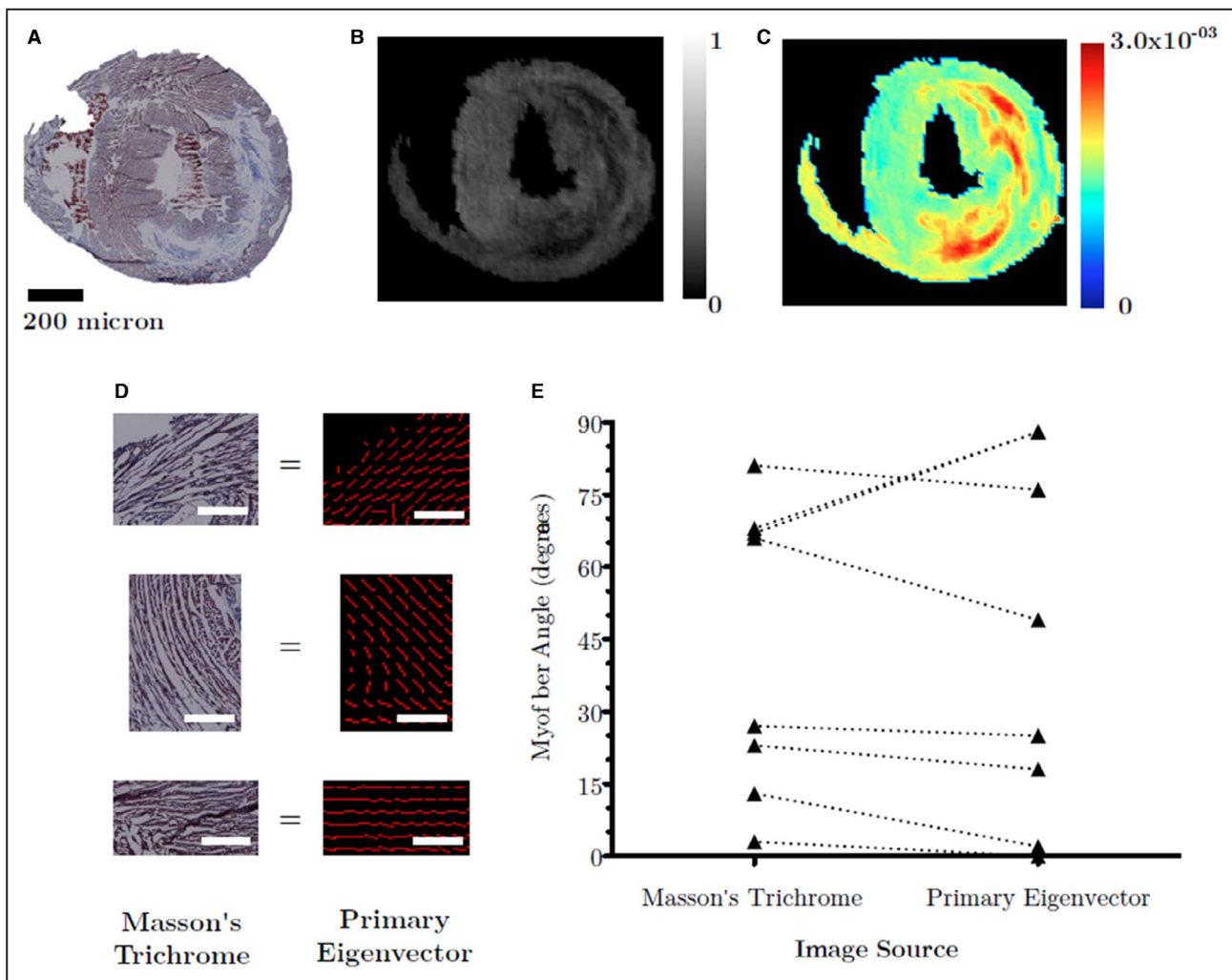†$P<0.05$ vs APD$_{50}$ in remote region of rotigaptide-treated.

Figure 5. Correlation of MR parameters and histology.
A, Regions of collagen deposition on Masson's trichrome–stained histological section and (**B**) areas of low fractional anisotropy and (**C**) areas of high mean diffusivity from a single section through the mid-LV of an infarcted heart. **D**, Three paired sections of normal myocardium showing (left) histology and (right) 2-dimensional primary eigenvector. Scale bar (white)=500 µm. (**E**) Comparison of orientation in normal myocardium between histology and primary eigenvector. LV indicates left ventricle; and MR, magnetic resonance.

(left-handed helix, −90°) through the LV wall in all hearts. In control hearts, the rate of change of HA through the LV wall (the slope of the linear fitted line) was similar in remote and IBZ regions (remote −157±5 versus IBZ −158±4, P=ns) with the transition point (the point at which the linear fitted line crosses zero degrees) significantly closer to the endocardium in the IBZ compared with remote (IBZ 65% versus remote 70%, $P<0.0001$, with transmural distance ranging from endocardium [0%] to epicardium [100%]). Similar findings were demonstrated in remote and IBZ regions of rotigaptide-treated hearts with no difference in rate of change of HA through the LV wall and a significantly more endocardial transition point in the IBZ region (Figure 7).

Transverse angle (TA) and transverse angle dispersion were comparable in the remote regions of control and rotigaptide-treated hearts (mean TA: CON 13±1°

versus 14±1°, ns, mean transverse angle dispersion: 9±1° versus 9±1°, ns). Rotigaptide had a significant effect on remodeling within the IBZ with a reduction in mean TA compared with CON (19±1 versus 16±1, P=0.013) and a reduction in mean transverse angle dispersion (10±1° versus 12±1°, P=0.015).

DISCUSSION

This study describes the effects of 7-day acute rotigaptide administration in a rat model of infarction–reperfusion on the electrophysiological and structural remodeling determined at 4 weeks post-MI. Rotigaptide did not reduce infarct size, but reduced fiber angular deviation in the adjacent region and reduced histomorphometric inhomogeneities in the IBZ associated with a reduction in ex vivo programmed electrical stimulation
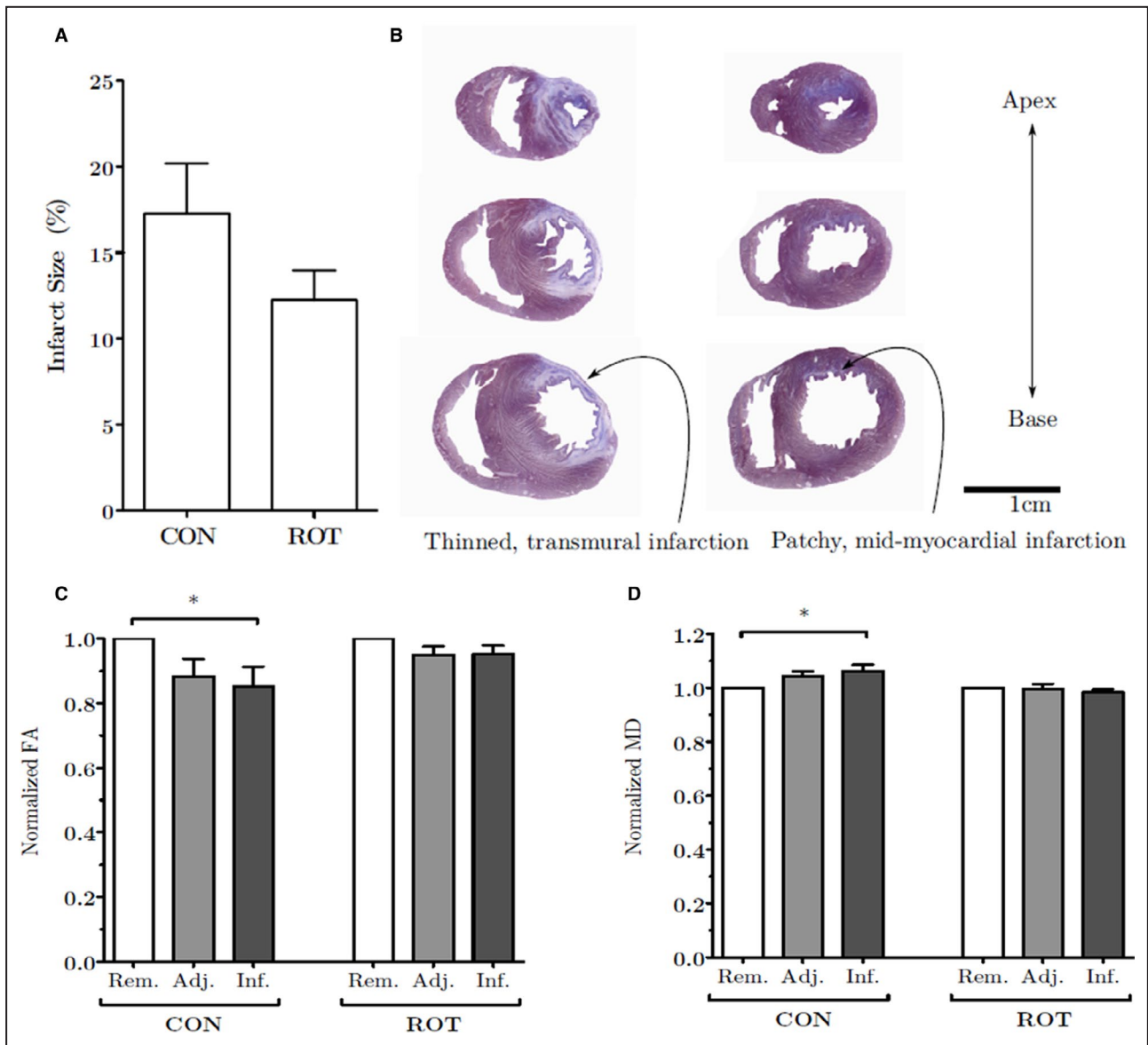
Figure 6.   The effect of rotigaptide on diffusion tensor MRI-derived measures of tissue architecture.
A, Infarct size, **B**, Histological representations, **C**, FA and **D,** MD. CON indicates MI+control (n=4); FA, fractional anisotropy; IBZ, infarct border zone; Inf, infarct; MD, mean diffusivity; Rem, remote; and ROT, MI+rotigaptide (n=3). *$P<0.05$.

(PES)–induced arrhythmias after 4 weeks despite no alteration in resting ECG, the incidence of in vivo spontaneous arrhythmias, or overall mortality.

In seeking potential explanations for the reduced inducibility of VT/VF in rotigaptide-treated hearts, the other novel findings of this study were that diffusion tensor imaging revealed that rotigaptide partially reversed indices of adverse structural remodeling with restoration of MR-defined anisotropy and diffusivity in the infarct region, relative to remote. In addition, examining the 3-dimensional structure of infarcted myocardium with diffusion tensor imaging offers a potential mechanistic explanation for the reduced inducibility of arrhythmias in rotigaptide-treated hearts.

Effect of Rotigaptide on Arrhythmogenesis and Electrophysiology

In this model, ECG parameters in the healed phase of reperfused infarction were similar between groups. This is in keeping with expectations considering the specific effect of rotigaptide only on GJ conductance, with little effect on membrane ionic currents.[41] Although the incidence of spontaneous arrhythmias in the healed phase was similar (and low) between groups, nevertheless, rotigaptide treatment afforded a reduction in arrhythmia score on PES, driven primarily by a reduction in inducibility when subject to ex vivo arrhythmia susceptibility testing. Re-entry is the
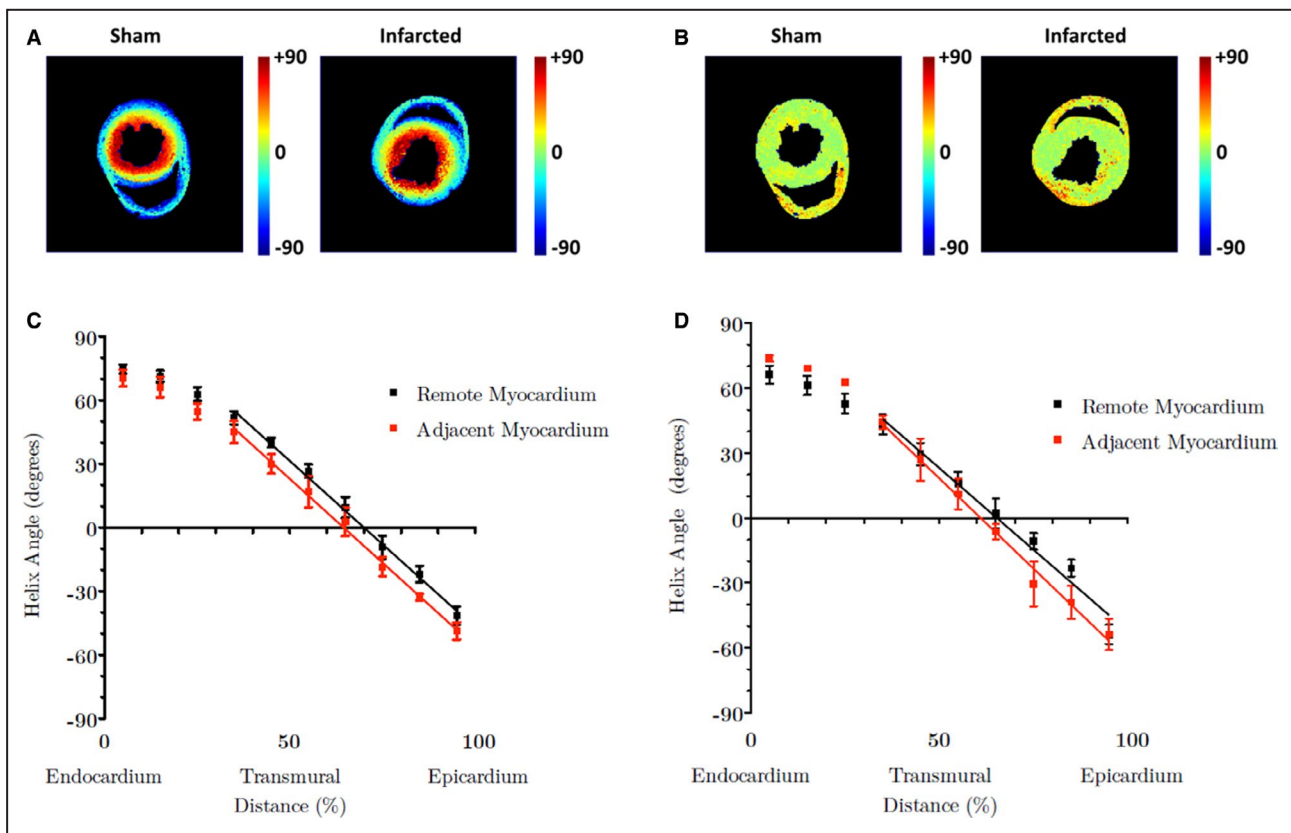
Figure 7. **Effect of rotigaptide treatment on 3-dimensional myocardial structure derived from diffusion tensor imaging.**
Representative single short-axis slice maps of (**A**) helix angle and (**B**) transverse angle in sham-operated and infarcted (no drug) hearts. Helix angle transitions from right-handed, positive angle in endocardial fibers to a left-handed, negative angle in epicardial fibers with a similar pattern in remote and infarct border zone regions of control (**C**) and rotigaptide-treated (**D**) hearts.

primary mechanism of PES-induced arrhythmias[42] and requires formation of a circuit with unidirectional block, slow conduction, and critical timing in order for re-entry to initiate and sustain. The reduction in arrhythmias induced by PES in the rotigaptide treatment group suggests that rotigaptide attenuates the negative electrophysiological or structural sequelae of infarction, resulting in hearts unable to sustain arrhythmogenesis. Modification of cellular electrophysiology did not mediate this attenuation. The magnitude of the reduction in conduction slowing at the IBZ was similar between groups, as was the degree of conduction dispersion, suggesting that the anti-arrhythmic effect of rotigaptide was not mediated by a change in the myocardial conduction properties at the border zone. Upstroke kinetics of the cardiac action potential were also similar between groups, lending further support to the GJ conductance-specific effect of rotigaptide. This is in contrast to our previous findings in permanent MI (not reperfused) where conduction slowing in the IBZ was attenuated with rotigaptide administration.[15]

In considering the mechanism of re-entrant ventricular arrhythmias, Allessie[43] showed that re-entry could arise because of differences in the recovery of excitability of tissue within the re-entrant circuit. Although some debate exists as to whether there is a true transmural repolarization gradient in the intact heart,[44] there is a wealth of experimental data that suggest that APD gradients exist in models of disease and contribute towards arrhythmogenesis in models of infarction[45] and heart failure.[46] The demonstration in this study of an APD50 gradient between the infarct region and remote region offers a putative mechanistic explanation for the development of ventricular arrhythmias because the increased dispersion provides the conditions necessary for re-entry arrhythmias to initiate and sustain and is in agreement with previous experimental models of infarction. Thollon et al first showed APD prolongation (at 25%, 50%, 75%, and 90%) in hypertrophied rat myocytes 4 weeks post-MI.[47] This was corroborated by Qin et al,[48] also in isolated rat myocytes at 4 weeks post-MI with prolongation of APD 50%, 75%, and 90%. They performed elegant patch-clamp studies that attributed APD remodeling to a significant decrease in density in both I_{tof} and I_{tos} currents with no alteration in calcium-handling kinetics. The presence of APD prolongation and a repolarization gradient between infarcted and remote myocardium were

associated with a significant increase in arrhythmia vulnerability, in agreement with the results in this study.

Effect of Rotigaptide on Infarct Size

There was no significant reduction in infarct size measured by planimetry consistent with our previous work[49] using the chronic-MI model of infarction but in contrast with Haugan et al.[23] These investigators demonstrated a significant reduction in infarct size in a rat model of chronic MI with a comparable dose of rotigaptide, but importantly their chronic MI model produces a consistent, thinned, transmural infarct across all treatment groups. This is in contrast to the infarction–reperfusion model, which produces a broader spectrum of infarct morphology ranging from patchy, discrete fibrosis to transmural, thinned infarction. Furthermore, Haugan et al pretreated rats with rotigaptide, to ensure a therapeutic concentration of rotigaptide at the time of left anterior descending artery occlusion. This is in contrast to the more clinically translational administration of rotigaptide after left anterior descending artery ligation in the present study. Large-animal studies using either rotigaptide[21] or danegaptide[50] in the acute setting of myocardial infarction–reperfusion have demonstrated reductions in infarct size when measured early (up to 4 hours). However, measurement of infarct size at this early time point represents area-at-risk, not healed scar, because the necrotic phase is incomplete and the reparative and healing phases have yet to start.

Structural Remodeling Induced by Rotigaptide

Changes in infarct heterogeneity, independent of infarct size, is a potential mechanistic explanation for the reduction in PES-inducible arrhythmias in the rotigaptide treatment group.[49] We previously described detailed histomorphometry of rat IBZ[15] showing that short-term enhancement of GJ function during acute MI modifies the healed arrhythmogenic substrate by reducing inhomogeneities of fibrosis at the healed border zone without gross changes in infarct size, thus reducing VT/VF inducibility late post-MI. In the current study this is manifest as attenuation/prevention of the relative reduction in FA (representing tissue structure) and increase in MD (representing cell structure) in the infarct region of control hearts resulting, in FA and MD values comparable to those of remote myocardium. A reduction in FA and increase in MD in the infarct region of the healed rat myocardium has been previously demonstrated by Chen et al,[24] attributed to the replacement of viable myocytes by loose strands of collagen that allow greater transverse diffusion and infiltration of inflammatory cells in the infarct region. These cells possess a more spherical cell shape, compared with the rodlike shape of normal myocytes. By contrast, the findings of Strijkers et al[51] showed an increase in FA post-MI, and this was attributed to the structured nature of collagen fibers.

It is possible that rotigaptide therapy has an intermediate effect on collagen deposition, with an increase in collagen density of sufficient magnitude to render diffusion equal in magnitude and anisotropy to remote myocardium, but of insufficient magnitude to replicate the findings of Strijkers et al.[51] An alternative explanation is the presence in rotigaptide-treated hearts of greater surviving strands or islands of myocytes within the infarct region, so as to result in a partial volume effect whereby the measured FA and MD are a reflection of both reduced anisotropy and increased diffusivity in areas of collagen deposition, offset against preserved anisotropy and normal diffusivity in areas with surviving myocytes.

The transmural course and mean values of helix and transverse angles are in agreement with those reported in the literature.[24] In healthy rat myocardium, helix angle values and transmural course are similar in anterior, lateral, septal, and inferior regions, and, as demonstrated, do not show a significant base-to-apex gradient.[24] In the 4-week chronic MI model of Chen et al,[24] the infarct region exhibited a greater change in HA per millimeter through the LV wall, because of its thinned nature, but when plotted as a function of transmural distance showed no significant change from remote myocardium. In this current study, the adjacent region did not demonstrate significant thinning, and showed a rate of change (ie, slope of linear fitted line) comparable to the remote region. However, the point of transition of the HA (through zero degrees) appeared to occur ≈5% (of total LV wall thickness) closer to the endocardium, with similar findings in both control and rotigaptide-treated groups. This shift in transition point is in keeping with the study of Rutherford et al,[52] who, in a high-resolution histological study of the IBZ, demonstrated that the normal pattern of transmural myofiber rotation was disrupted across the IBZ with a shift in transition point towards the endocardium. HA deviation, a marker of fiber orientation coherence, was similar in remote and adjacent regions in both treatment groups, with sporadic differences between remote and adjacent regions only present in the midmyocardium (45%–65% of transmural distance) of control-treated hearts. The mean HA deviation of 14° in the remote region is higher than the 10° reported by Chen et al,[24] with the 16° in the adjacent region lower than the 20° reported in the infarct region, although discrepancies in values likely reflect differences in the segmentation of myocardium between studies.

In this study we have shown that the TA, the component of the myofiber orientation in the x-y plane, was similar in remote regions of control and rotigaptide-treated hearts and was significantly higher in the adjacent regions of both when compared with respective remote regions. However, the mean TA in the adjacent region was significantly reduced in the rotigaptide-treated group, compared with the adjacent region of control hearts, suggesting a more ordered and tightly packed orientation of myofibers. TA deviation, another marker of fiber orientation coherence, was significantly higher in adjacent regions of control hearts in comparison to remote regions, a finding that was not replicated in the rotigaptide-treated group, which instead demonstrated restoration of TA deviation in the adjacent region to values seen in remote myocardium. The reduced mean TA and reduced deviation of myofibers in the x-y plane in the adjacent region of rotigaptide-treated hearts may reflect a more ordered healing process and offers a putative mechanistic explanation for the reduced arrhythmogenesis by creating a more homogeneous, less arrhythmia-prone border zone.

Limitations

Optical action potential and calcium transient analysis was constrained to the visible epicardial surface and was divided into 3 regions based on the Complementary Metal–Oxide–Semiconductor image appearance. It is conceivable, however, that within each region (specifically the IBZ and infarct) there may exist significant interregional variability, particularly in APD, which, because of the spatial resolution of analysis, may not be appreciated. This interregional variability may unmask areas of local heterogeneity, which may offer a mechanistic explanation of arrhythmogenicity whereas averaged, large, regional-based analysis would appear to show little heterogeneity.

Because of the number of hearts undergoing diffusion tensor imaging, it was not possible to perform subgroup analyses of arrhythmic versus nonarrhythmic hearts to determine whether diffusion imaging could identify hearts with high arrhythmic risk. Although rotigaptide treatment appeared to confer significant remodeling benefit in the form of restoring FA and MD in the infarct region to values of the remote region and in reducing the variation in fiber orientation in the adjacent region, it is not possible to comment on whether these changes rendered individual hearts less or more susceptible to arrhythmogenesis.

With regard to the diffusion-MRI-derived indices, only the remote and adjacent regions were analyzed, because of the variable degree of wall thinning demonstrated in the infarct region and the potential partial volume effect in attempting to divide the infarct region into deciles.

MRI diffusion indices may be affected by regional myocardial differences even in normal hearts.[53] For this reason control and rotigaptide values were compared within the same myocardial regions.

The number of animals in each group for the measurements of FA and MD were small, limiting the ability to identify a statistically significant difference with/without rotigaptide.

CONCLUSIONS

Early enhancement of GJ coupling after infarction–reperfusion injury leads to reduced susceptibility to PES-induced arrhythmias, and is associated with restoration of structural anisotropy and diffusivity. This demonstrates the potential therapeutic value of rotigaptide treatment alongside reperfusion strategies in acute management of post-MI.

REFERENCES

1. Sarter BH, Finkle JK, Gerszten RE, Buxton AE. What is the risk of sudden cardiac death in patients presenting with hemodynamically stable sustained ventricular tachycardia after myocardial infarction? *J Am Coll Cardiol*. 1996;28:122–129. DOI: 10.1016/0735-1097(96)00123-4.
2. de Bakker JM, van Capelle FJ, Janse MJ, Tasseron S, Vermeulen JT, de Jonge N, Lahpor JR. Slow conduction in the infarcted human heart. "Zigzag" course of activation. *Circulation*. 1993;88:915–926. DOI: 10.1161/01.CIR.88.3.915.

3. Kaplinsky E, Horowitz A, Neufeld HN. Ventricular reentry and automaticity in myocardial infarction. Effect of size of injury. *Chest*. 1978;74:66–71. DOI: 10.1378/chest.74.1.66.

4. Bolick DR, Hackel DB, Reimer KA, Ideker RE. Quantitative analysis of myocardial infarct structure in patients with ventricular tachycardia. *Circulation*. 1986;74:1266–1279. DOI: 10.1161/01.CIR.74.6.1266.

5. Schmidt André, Azevedo CF, Cheng A, Gupta SN, Bluemke DA, Foo TK, Gerstenblith G, Weiss RG, Marbán E, Tomaselli GF, et al. Infarct tissue heterogeneity by magnetic resonance imaging identifies enhanced cardiac arrhythmia susceptibility in patients with left ventricular dysfunction. *Circulation*. 2007;115:2006–2014. DOI: 10.1161/CIRCULATIONAHA.106.653568.

6. CAST. Preliminary report: effect of encainide and flecainide on mortality in a randomized trial of arrhythmia suppression after myocardial infarction. The Cardiac Arrhythmia Suppression Trial (CAST) Investigators. *N Engl J Med*. 1989;321:406–412. DOI: 10.1056/NEJM198908103210629.

7. Cairns JA, Connolly SJ, Roberts R, Gent M. Randomised trial of outcome after myocardial infarction in patients with frequent or repetitive ventricular premature depolarisations: CAMIAT. Canadian Amiodarone Myocardial Infarction Arrhythmia Trial Investigators. *Lancet*. 1997;349:675–682. DOI: 10.1016/S0140-6736(96)08171-8.

8. Freemantle N, Cleland J, Young P, Mason J, Harrison J. beta Blockade after myocardial infarction: systematic review and meta regression analysis. *BMJ*. 1999;318:1730–1737. DOI: 10.1136/bmj.318.7200.1730.

9. Russo AM, Stainback RF, Bailey SR, Epstein AE, Heidenreich PA, Jessup M, Kapa S, Kremers MS, Lindsay BD, Stevenson LW. ACCF/HRS/AHA/ASE/HFSA/SCAI/SCCT/SCMR 2013 appropriate use criteria for implantable cardioverter-defibrillators and cardiac resynchronization therapy. *Hear Rhythm*. 2013;10:e11–e58. DOI: 10.1016/j.hrthm.2013.01.008.

10. Sanders GD, Hlatky MA, Owens DK. Cost-effectiveness of implantable cardioverter-defibrillators. *N Engl J Med*. 2005;353:1471–1480. DOI: 10.1056/NEJMsa051989.

11. Ng FS, Holzem KM, Koppel AC, Janks D, Gordon F, Wit AL, Peters NS, Efimov IR. Adverse remodeling of the electrophysiological response to ischemia-reperfusion in human heart failure is associated with remodeling of metabolic gene expression. *Circ Arrhythm Electrophysiol*. 2014;7:875–882. DOI: 10.1161/CIRCEP.113.001477.

12. Rohr S. Role of gap junctions in the propagation of the cardiac action potential. *Cardiovasc Res*. 2004;62:309–322. DOI: 10.1016/j.cardiores.2003.11.035.

13. Peters NS, Wit AL. Gap junction remodeling in infarction: does it play a role in arrhythmogenesis? *J Cardiovasc Electrophysiol*. 2000;11:488–490. DOI: 10.1111/j.1540-8167.2000.tb00348.x.

14. Peters NS, Coromilas J, Severs NJ, Wit AL. Disturbed connexin43 gap junction distribution correlates with the location of reentrant circuits in the epicardial border zone of healing canine infarcts that cause ventricular tachycardia. *Circulation*. 1997;95:988–996. DOI: 10.1161/01.CIR.95.4.988.

15. Ng FS, Kalindjian JM, Cooper SA, Chowdhury RA, Patel PM, Dupont E, Lyon AR, Peters NS. Enhancement of gap junction function during acute myocardial infarction modifies healing and reduces late ventricular arrhythmia susceptibility. *JACC Clin Electrophysiol*. 2016;2:574–582. DOI: 10.1016/j.jacep.2016.03.007.

16. Garcia-Dorado D. Gap junction-mediated spread of cell injury and death during myocardial ischemia-reperfusion. *Cardiovasc Res*. 2004;61:386–401. DOI: 10.1016/j.cardiores.2003.11.039.

17. Decrock E, Vinken M, De Vuyst E, Krysko DV, D'Herde K, Vanhaecke T, Vandenabeele P, Rogiers V, Leybaert L. Connexin-related signaling in cell death: to live or let die? *Cell Death Differ*. 2009;16:524–536. DOI: 10.1038/cdd.2008.196.

18. Kjølbye AL, Knudsen CB, Jepsen T, Larsen BD, Petersen JS. Pharmacological characterization of the new stable antiarrhythmic peptide analog Ac- D -Tyr- D -Pro- D -Hyp-Gly- D - Ala-Gly-NH 2 (ZP123). In vivo and in vitro studies. *J Pharmacol Exp Ther*. 2003;306:1191–1199. DOI: 10.1124/jpet.103.052258.

19. Butera JA, Larsen BD, Hennan JK. Discovery of (2 S, 4 R)-1-(2-Aminoacetyl)-4-benzamidopyrrolidine-2-carboxylic acid hydrochloride (GAP-134) 13, an orally active small molecule gap-junction modifier for the treatment of atrial fibrillation. *J Med Chem*. 2009;52:908–911. DOI: 10.1021/jm801558d.

20. Hennan JK, Swillo RE, Morgan GA, Keith JC, Schaub RG, Smith RP, Feldman HS, Haugan K, Kantrowitz J, Wang PJ, et al. Rotigaptide (ZP123) prevents spontaneous ventricular arrhythmias and reduces infarct size during myocardial ischemia/reperfusion injury in open-chest dogs. *J Pharmacol Exp Ther*. 2006;317:236–243. DOI: 10.1124/jpet.105.096933.

21. Hennan JK, Swillo RE, Morgan GA, Rossman EI, Kantrowitz J, Butera J, Petersen JS, Gardell SJ, Vlasuk GP. GAP-134 ([2S,4R]-1-[2-aminoacetyl]4-benzamidopyrrolidine-2-carboxylic acid) prevents spontaneous ventricular arrhythmias and reduces infarct size during myocardial ischemia/reperfusion injury in open-chest dogs. *J Cardiovasc Pharmacol Ther*. 2009;14:207–214. DOI: 10.1177/1074248409340779.

22. Axelsen LN, Stahlhut M, Mohammed S, Larsen BD, Nielsen MS, Holstein-Rathlou N-H, Andersen S, Jensen ON, Hennan JK, Kjølbye AL. Identification of ischemia-regulated phosphorylation sites in connexin43: a possible target for the antiarrhythmic peptide analogue rotigaptide (ZP123). *J Mol Cell Cardiol*. 2006;40:790–798. DOI: 10.1016/j.yjmcc.2006.03.005.

23. Haugan K, Marcussen N, Kjølbye AL, Nielsen MS, Hennan JK, Petersen JS. Treatment with the gap junction modifier rotigaptide (ZP123) reduces infarct size in rats with chronic myocardial infarction. *J Cardiovasc Pharmacol*. 2006;47:236–242. DOI: 10.1097/01.fjc.0000200990.31611.6e.

24. Chen J, Song S-K, Liu W, McLean M, Allen JS, Tan J, Wickline SA, Yu X. Remodeling of cardiac fiber structure after infarction in rats quantified with diffusion tensor MRI. *Am J Physiol Heart Circ Physiol*. 2003;285:H946–H954. DOI: 10.1152/ajpheart.00889.2002.

25. Wu Y, Tse H-F, Wu EX. Diffusion tensor MRI study of myocardium structural remodeling after infarction in porcine model. *Conf Proc IEEE Eng Med Biol Soc*. 2006;1:1069–1072. DOI: 10.1109/IEMBS.2006.259840.

26. Wu MT, Su MYM, Huang YL, Chiou KR, Yang P, Pan HB, Reese TG, Wedeen VJ, Tseng WYI. Sequential changes of myocardial microstructure in patients postmyocardial infarction by diffusion-tensor cardiac MR: correlation with left ventricular structure and function. *Circ Cardiovasc Imaging*. 2009;2:32–40. DOI: 10.1161/CIRCIMAGING.108.778902.

27. Wu M-T, Tseng W-YI, Su M-YM, Liu C-P, Chiou K-R, Wedeen VJ, Reese TG, Yang C-F. Diffusion tensor magnetic resonance imaging mapping the fiber architecture remodeling in human myocardium after infarction: correlation with viability and wall motion. *Circulation*. 2006;114:1036–1045. DOI: 10.1161/CIRCULATIONAHA.105.545863.

28. Wu EX, Wu Y, Nicholls JM, Wang J, Liao S, Zhu S, Lau C-P, Tse H-F. MR diffusion tensor imaging study of postinfarct myocardium structural remodeling in a porcine model. *Magn Reson Med*. 2007;58:687–695. DOI: 10.1002/mrm.21350.

29. Deloche A, Fabiani JN, Camilleri JP, Relland J, Joseph D, Carpentier A, Dubost C. The effect of coronary artery reperfusion on the extent of myocardial infarction. *Am Heart J*. 1977;93:358–366. DOI: 10.1016/S0002-8703(77)80255-X.

30. Curtis MJ, Walker MJ. Quantification of arrhythmias using scoring systems: an examination of seven scores in an in vivo model of regional myocardial ischaemia. *Cardiovasc Res*. 1988;22:656–665. DOI: 10.1093/cvr/22.9.656.

31. Kmecova J, Klimas J. Heart rate correction of the QT duration in rats. *Eur J Pharmacol*. 2010;641:187–192. DOI: 10.1016/j.ejphar.2010.05.038.

32. Bell RM, Mocanu MM, Yellon DM. Retrograde heart perfusion: the Langendorff technique of isolated heart perfusion. *J Mol Cell Cardiol*. 2011;50:940–950. DOI: 10.1016/j.yjmcc.2011.02.018.

33. Lyon AR, Bannister ML, Collins T, Pearce E, Sepehripour AH, Dubb SS, Garcia E, O'Gara P, Liang L, Kohlbrenner E, et al. SERCA2a gene transfer decreases sarcoplasmic reticulum calcium leak and reduces ventricular arrhythmias in a model of chronic heart failure. *Circ Arrhythm Electrophysiol*. 2011;4:362–372. DOI: 10.1161/CIRCEP.110.961615.

34. Nguyen T, el Salibi E, Rouleau JL. Postinfarction survival and inducibility of ventricular arrhythmias in the spontaneously hypertensive rat: effects of ramipril and hydralazine. *Circulation*. 1998;98:2074–2080. DOI: 10.1161/01.CIR.98.19.2074.

35. Efimov IR, Nikolski VP, Salama G. Optical imaging of the heart. *Circ Res*. 2004;95:21–33. DOI: 10.1161/01.RES.0000130529.18016.35.

36. Laughner JI, Ng FS, Sulkin MS, Arthur RM, Efimov IR. Processing and analysis of cardiac optical mapping data obtained with potentiometric dyes. *Am J Physiol Heart Circ Physiol*. 2012;303:H753–H765. DOI: 10.1152/ajpheart.00404.2012.

37. Jones DK, Horsfield MA, Simmons A. Optimal strategies for measuring diffusion in anisotropic systems by magnetic resonance imaging. *Magn Reson Med*. 1999;42:515–525. DOI: 10.1002/(SICI)1522-2594(199909)42:3<515:AID-MRM14>3.0.CO;2-Q.

38. Wang R, Benner T, Sorensen AG, Wedeen VJ. Diffusion toolkit: a software package for diffusion imaging data processing and tractography. *Proc Int Soc Mag Reson Med*. 2007;15:3720.

39. Geerts L, Bovendeerd P, Nicolay K, Arts T. Characterization of the normal cardiac myofiber field in goat measured with MR-diffusion tensor imaging. *Am J Physiol Heart Circ Physiol*. 2002;283:H139–H145. DOI: 10.1152/ajpheart.00968.2001.

40. Scollan DF, Holmes A, Winslow R, Forder J. Histological validation of myocardial microstructure obtained from diffusion tensor magnetic resonance imaging. *Am J Physiol*. 1998;275:H2308–H2318. DOI: 10.1152/ajpheart.1998.275.6.H2308.

41. Xing DZ, Kjolbye AL, Nielsen MS, Petersen JS, Harlow KW, Holstein-Rathlou NH, Martins JB. ZP123 increases gap junctional conductance and prevents Reentrant ventricular tachycardia during myocardial ischemia in open chest dogs. *J Cardiovasc Electrophysiol*. 2003;14:510–520. DOI: 10.1046/j.1540-8167.2003.02329.x.

42. Wellens HJ. Value and limitations of programmed electrical stimulation of the heart in the study and treatment of tachycardias. *Circulation*. 1978;57:845–853. DOI: 10.1161/01.CIR.57.5.845.

43. Allessie MA, Bonke FI, Schopman FJ. Circus movement in rabbit atrial muscle as a mechanism of tachycardia. II. The role of nonuniform recovery of excitability in the occurrence of unidirectional block, as studied with multiple microelectrodes. *Circ Res*. 1976;39:168–177. DOI: 10.1161/01.RES.39.2.168.

44. Opthof T, Coronel R, Janse MJ. Is there a significant transmural gradient in repolarization time in the intact heart?: Repolarization gradients in the intact heart. *Circ Arrhythm Electrophysiol*. 2009;2:89–96. DOI: 10.1161/CIRCEP.108.825356.

45. Wong SS, Bassett AL, Cameron JS, Epstein K, Kozlovskis P, Myerburg RJ. Dissimilarities in the electrophysiological abnormalities of lateral border and central infarct zone cells after healing of myocardial infarction in cats. *Circ Res*. 1982;51:486–493. DOI: 10.1161/01.RES.51.4.486.

46. Akar FG, Rosenbaum DS. Transmural electrophysiological heterogeneities underlying arrhythmogenesis in heart failure. *Circ Res*. 2003;93:638–645. DOI: 10.1161/01.RES.0000092248.59479.AE.

47. Thollon C, Kreher P, Charlon V, Rossi A. Hypertrophy induced alteration of action potential and effects of the inhibition of angiotensin converting enzyme by perindopril in infarcted rat hearts. *Cardiovasc Res*. 1989;23:224–230. DOI: 10.1093/cvr/23.3.224.

48. Qin D, Zhang ZH, Caref EB, Boutjdir M, Jain P, El-Sherif N. Cellular and ionic basis of arrhythmias in postinfarction remodeled ventricular myocardium. *Circ Res*. 1996;79:461–473. DOI: 10.1161/01.RES.79.3.461.

49. Ng FS, Kalindjian JM, Cooper SA, Chowdhury RA, Patel PM, Roney CH, Dupont E, Lyon AR, Peters NS. Abstract 10654: enhancement of gap junctional coupling during acute myocardial infarction reduces inhomogeneity of border zone scarring and late ventricular arrhythmia susceptibility. *Circulation*. 2011;124:A10654.

50. Skyschally A, Walter B, Hansen RS, Heusch G. The antiarrhythmic dipeptide ZP16069 (danegaptide) when given at reperfusion myocardial infarct size in pigs. *J Am Coll Cardiol*. 2013;61:E67. DOI: 10.1007/s0021 0-013-0840-9.

51. Strijkers GJ, Bouts A, Blankesteijn WM, Peeters THJM, Vilanova A, van Prooijen MC, Sanders HMHF, Heijman E, Nicolay K. Diffusion tensor imaging of left ventricular remodeling in response to myocardial infarction in the mouse. *NMR Biomed*. 2009;22:182–190. DOI: 10.1002/nbm.1299.

52. Rutherford SL, Trew ML, Sands GB, Legrice IJ, Smaill BH. High-resolution 3-dimensional reconstruction of the infarct border zone: impact of structural remodeling on electrical activation. *Circ Res*. 2012;111:301–311. DOI: 10.1161/CIRCRESAHA.111.260943.

53. McGill L-A, Scott AD, Ferreira PF, Nielles-Vallespin S, Ismail T, Kilner PJ, Gatehouse PD, De Silva R, Prasad SK, Giannakidis A, et al. Heterogeneity of fractional anisotropy and mean diffusivity measurements by in vivo diffusion tensor imaging in normal human hearts. *PLoS One*. 2015;10:1–17. DOI: 10.1371/journal.pone.0132360.

SUPPLEMENTAL MATERIAL

Data S1.

Supplemental Methods

Ethical and Home Office Approval
All animal procedures were performed in accordance with the standards set out in the UK Animals (Scientific Procedures) Act 1986 with appropriate PPL (70/7419), PIL (70/24061) permissions and subject to local ethical review.

Surgical Model of Infarction-Reperfusion
Thirty seven male Sprague-Dawley rats (weight 250-350g) underwent myocardial infarction-reperfusion (MI) surgery. Briefly, rats were anaesthetised using vaporised Isoflurane then intubated and ventilated using a positive pressure ventilator. The left lateral chest area was shaved and prepped with Povidone Iodine and a dose of Buprenorphine (5mg/kg sc) and Enrofloxacin (0.05mg/kg) administered pre-operatively. A 4cm vertical incision was made over the left lateral chest area and a thoracotomy performed between the 3rd and 4th intercostal spaces to expose the heart. The pericardium was divided and the thymus retracted cranially to expose the anterior surface of the heart and allow visualisation of the left anterior descending (LAD). A 6-0 monofilament suture was looped around the proximal LAD and a slipknot tightened to induce infarction or removed in sham-operated animals. Successful occlusion of the LAD was confirmed by blanching of the myocardium and regional LV wall hypokinesis. The free ends of the slipknot were externalised and the intercostals, pectoralis and skin closed with 4-0 silk. Free air was expelled from the chest using a positive pressure cycle and animals extubated and maintained on a Bain coaxial anaesthetic mask with inhaled Isoflurane (2%). After 60 minutes of LAD occlusion the free ends of the slipknot were pulled to allow release of the knot and restore coronary flow. The rats were recovered in a hotbox and monitored post-operatively until the end of the study protocol.

Drug Administration
Rats were randomly divided into two groups at the time of MI surgery; a control group that received phosphate-buffered saline (PBS) and a treatment group that received the gap junction enhancing drug Rotigaptide. At 15 minutes post-LAD occlusion, prior to reperfusion, rats received either Rotigaptide (2.5mol/kg) or PBS (1ml) via intraperitoneal injection. Following reperfusion animals were treated for a week using an osmotic minipump (Azlet Minipump 2ML1) filled with either PBS (at a rate of 2ml/week) or Rotigaptide (at a rate of 0.11nmol/kg/day). The osmotic minipump was implanted in the abdominal cavity following reperfusion by making a small vertical abdominal incision along the linea alba and dividing the anterior abdominal wall muscles to form a laparotomy. After placing the minipump inside the abdominal cavity the abdominal muscles and skin layers were closed with 4-0 silk.

In Vivo ECG Telemetry Recordings
The incidence of spontaneous ventricular arrhythmias was measured with an implantable wireless ECG telemetry transmitter (CA-F40, DataSciences). At seven days post-MI rats were anaesthetised using vaporised Isoflurane (2%), maintained on a Bain co-axial system with inhaled Isoflurane (2%) and the abdominal area shaved, prepped with Povidone Iodine and a dose of Buprenorphine (5mg/kg sc) and Enrofloxacin (0.05mg/kg) administered pre-operatively. A vertical abdominal incision was made along the linea alba and the anterior abdominal wall muscles divided to form a laparotomy. The osmotic minipump implanted at the time of MI surgery was

removed and the body of the wireless transmitter sutured to the anterior abdominal wall using a 4-0 silk suture. The two bio-potential leads were positioned in a pseudo-lead II position with the positive lead tunnelled subcutaneously and secured under the cardiac apex and the negative lead tunnelled subcutaneously and secured in the right axilla. Animals were recovered in a hot box prior to being individually housed in a custom-built telemetry rack (Technoplastics) and the implanted transmitter paired to a receiver-plate positioned under each cage. Continuous ECG recordings were performed for a 72 hour period at 28 days post-MI surgery. From this dataset, a 24 hour window of data, in time with the light-dark cycle of the animal facility was extracted and the number of ventricular premature beats (VPB), number of runs of ventricular tachycardia (VT) and number of runs of ventricular fibrillation (VF) quantified by semi-automatic analysis (EMKA ECG Software) and a composite arrhythmia score calculated [Curtis Ref]

Score = log(Number of VPB) + log(Number of VT Episodes) + log(Number of VF Episodes)

In Vivo ECG Recordings
The resting ECG was recorded using a small-animal 6-lead ECG system (iWorx). At 28 days post-MI rats were anaesthetised using vaporised Isoflurane (5%) and maintained on a Bain co-axial system with inhaled Isoflurane (2%). Grass platinum sub-dermal needle electrodes were attached to each limb with a reference electrode attached to the right leg. Data were acquired at a sampling rate of 1KHz and bandpass filtered between 0.3-30Hz. Data were analysed offline (LabScribe 2, iWorx) to measure specific ECG intervals (PR, QRS, RR, QTc intervals, measured in milliseconds (ms)) averaged from 10 consecutive beats in the lead with greatest QRS amplitude.

Langendorff Perfusion Studies
At 28 days post-MI rats were sacrificed by an overdose of anaesthetic followed by cervical dislocation and the heart retrograde perfused with oxygenated Krebs-Henseleit buffer (composition Na, pH 7.35-7.45, temperature 36.5-37.5^{o}C) using a flow-driven Langendorff system (Radnoti) to give a perfusion pressure of 80-90mmHg. The heart was placed in a perspex, fluid filled chamber to facilitate optical mapping and a real-time field ECG recorded using an electrode placed in contact with the fluid in the chamber and a reference electrode connected to the aortic cannula. Cardiac pacing was achieved using a needle pacing electrode placed on the RV endocardium connected to a reconditioned clinical pacing system (MicroPace III) with a rectangular pulse at twice diastolic threshold and of duration 2ms. The heart was allowed to stabilise in sinus rhythm for 15 minutes prior to arrhythmia provocation and optical mapping studies

Arrhythmia Provocation Studies
The effects of Rotigaptide treatment on the susceptibility to arrhythmias induced by programmed stimulation was assessed using an extrastimulus programmed electrical stimulation (PES) protocol [ARL reference]. Briefly, hearts were subject to an S1S2 provocation protocol with a drivetrain of 10 S1 beats at CL 120ms followed by a single premature extrastimulus (S2) at a CL of 100ms, decrementing in 2ms steps until refractory or an induced arrhythmia occurred. If the heart remained in sinus rhythm a S1S2S3 protocol was performed with an additional extrastimulus (S3) at a CL of 80ms, decrementing in 2ms steps. Arrhythmias were defined in keeping

with the Lambeth conventions [REF] and quantified according to the score proposed by Nguyen (nil inducible = 0, NSVT on S1S2S3 = 1, Sustained VT on S1S2S3 = 2, NSVT on S1S2 = 3, Sustained VT on S1S2 = 4, NSVT or Sustained VT on S1 pacing = 5, NSVT or Sustained VT post stabilisation = 6).